

Nonexistence of Efficient Dominating Sets in the Cayley Graphs Generated by Transposition Trees of Diameter 3

ITALO J. DEJTER AND OSCAR TOMAICONZA

University of Puerto Rico
Rio Piedras, PR 00936-8377

e-mail: oscar.tomaiconza@hotmail.com

Abstract

Let d, n be positive integers such that $d < n$, and let X_n^d be a Cayley graph generated by a transposition tree of diameter d . It is known that every X_n^d with $d < 3$ splits into efficient dominating sets. The main result of this paper is that X_n^3 does not have efficient dominating sets.

Keywords: Cayley graph, efficient dominating set, sphere packing.

2010 Mathematics Subject Classification: 05C69; 05C70; 05C12.

1. INTRODUCTION

Cayley graphs are very important for their useful applications (cf. [10]), including to automata theory (cf. [11, 12]), interconnection networks (cf. [1, 2, 4, 5, 6]) and coding theory (cf. [3, 4]).

Let $0 < d < n$ in \mathbb{Z} , and let X_n^d be a Cayley graph generated by a transposition tree of diameter d . In [4], it was shown that every X_n^d with $d < 3$ splits into efficient dominating sets. In the present work, the following result is proved.

Theorem 1.1. *Let $3 < n$. Then no X_n^3 has efficient dominating sets.*

The rest of this section is devoted to preliminaries and a plan of our proof of Theorem 1.1. Let $0 < n \in \mathbb{Z}$ and let $I_n = \{1, 2, \dots, n\}$. Let S_n be the group of permutations $\sigma = \begin{pmatrix} 1 & \dots & n \\ \sigma_1 & \dots & \sigma_n \end{pmatrix} : I_n \rightarrow I_n$ with $\sigma(i) = \sigma_i$ for every $i \in I_n$ and $\{\sigma_1, \dots, \sigma_n\} = I_n$. We write $\sigma = \sigma_1 \cdots \sigma_n$. Thus, $e = 12 \cdots n$ means the identity of S_n . Let $\mathcal{C} \subseteq S_n \setminus \{e\}$ satisfy $\sigma \in \mathcal{C} \Leftrightarrow \sigma^{-1} \in \mathcal{C}$. The *Cayley graph* $X = X(S_n, \mathcal{C})$ of S_n with *connection set* \mathcal{C} is the graph $X = (S_n, E)$ with $gh \in E \Leftrightarrow h = \sigma g$, where $\sigma = hg^{-1} \in \mathcal{C}$. Here, if $\sigma = \sigma^{-1}$, we say that $gh \in E$ has *color* σ .

In [7], Lemma 3.7.4 shows that X is connected if and only if \mathcal{C} is a generating set for S_n , and Lemma 3.10.1 shows that a set of transpositions (ij) of S_n , with $i \neq j$ in I_n , generates S_n if and only if the graph τ whose edges are of the form ij is connected. We start Subsection 1.1 by considering such a graph τ .

1.1. Transpositions, Domination and Packing

Let τ be a connected graph with vertex set I_n and let $\mathcal{C} = \mathcal{C}_\tau$ be composed by the transpositions $\sigma = (ij)$, where ij runs over the edges of τ . Then $\sigma = \sigma^{-1}$ for each $\sigma \in \mathcal{C}_\tau$. This yields the graph $X(S_n, \tau) = X(S_n, \mathcal{C}_\tau)$ as an edge-colored graph via the *color set* \mathcal{C}_τ with a 1-factorization into the 1-factors $F_\sigma = F_{ij}$ of σ -colored edges. Here, τ is called the *transposition graph* of $X(S_n, \tau)$ [5, 6].

For domination and packing in Cayley graphs, the terminology of [8] is used. A *stable subset* $J \subseteq S_n$ (i.e. a set of nonadjacent vertices) with each vertex of $S_n \setminus J$ adjacent in the Cayley graph X to just one vertex of J is an *efficient dominating set* (or *E-set*) of X . The *1-sphere* with *center* $g \in S_n$ is the subset $\{h \in S_n \mid \rho(g, h) \leq 1\}$, where ρ is the graph distance of X . Every E-set in X is the set of centers of the 1-spheres in a *perfect sphere packing* (as in [9], page 109) of X . Let X' be a proper subgraph of X (X' specified in Subsection 1.4). Let \mathcal{S} be a perfect 1-sphere packing of X' . The union of a 1-sphere of \mathcal{S} with its neighbors in $S_n \setminus V(X')$ is an *\mathcal{S} -sphere*. The union of two 1-spheres centered at adjacent vertices x, x' of X is a *double-sphere* with *centers* x, x' . A collection of pairwise disjoint 1-spheres (resp., \mathcal{S} -spheres and double-spheres) in X is said to be a *1-sphere packing* of X (resp., a *special packing* of X , to be used in Section 6). It may happen that X has a packing \mathcal{T} by \mathcal{S} -spheres, see Figure 1 below.

Given a packing \mathcal{S} of 1-spheres in X whose union has cardinality $\alpha|S_n| = \alpha n!$, ($0 < \alpha \leq 1$), the set J of centers of the 1-spheres of \mathcal{S} is an α -*efficient dominating set* (or α -*E-set*) of X , in which case we may denote (by abuse of notation) the induced subgraph $X[J]$ by J . Note that a 1-E-set is an E-set, and viceversa.

1.2. Transposition Trees of Diameter less than 3

Theorem 3.10.2 [7] implies that \mathcal{C}_τ is a minimal generating set for $S_n \Leftrightarrow \tau$ is a tree. We take $\tau = \tau^{d_n} = \tau^d$ to be a diameter- d tree and denote $X_n^d = X(S_n, \tau^d)$. Let $\tau^{d_1} = \tau^0 = (I_1, \emptyset)$. Let $\tau^{d_n} = K_{1, n-1}$ with $d_n = 2$ if $n > 2$ and $d_n = 1$ if $n = 2$. By assuming $1 \in I_n = V(\tau^{d_n})$ of degree $n-1$, $S_n = V(X_n^{d_n})$ splits into E-sets $\xi_i^1 = i(I_n \setminus \{1\})$, ($i \in I_n$), formed by those $\sigma \in S_n$ with $\sigma_1 = i$ [2]. (For example, $\xi_1^1 = 1(2, \dots, n)$, also written as $\xi_1^1 = 1(2 \cdots n)$). In this terms, [4] showed that if $n > 1$ then for each $i \in I_n$, $X_n^{d_n} - \xi_i^1$ is the disjoint union of $n-1$ copies ξ_i^j of $X_{n-1}^{d_{n-1}}$, where ξ_i^j is induced by all $\sigma \in S_n$ with $\sigma_j = i$ and $j \in I_n \setminus \{1\}$. This is used in proving Theorem 1.1 as we indicate in Subsections 1.3 and 1.4.

1.3. Transposition Trees of Diameter 3

A diameter-3 tree τ^3 has two vertices of degrees r, t larger than 1 joined by an edge ϵ . Then $n = r + t$. We write $\tau^3 = \tau_{r,t}^3$ and take: (i) r and $r^* = r + 1$ as the vertices of $\tau_{r,t}^3$ of degrees r and t so that $\epsilon = rr^*$; (ii) $1, \dots, r-1$ (resp.,

$r^* + 1, \dots, n$) as the neighbors of r (resp., r^*) in $\tau_{r,t}^3$. (This vertex numbering is modified in Sections 7-8). Edge pairs in $\tau_{r,t}^3$ induce copies of both: **(A)** the disjoint union $2K_2 = 2P_2$ of two paths of length 1; **(B)** the path P_3 of length 2. Using two-color alternation in $X_{r,t}^3 = X(S_n, \tau_{r,t}^3)$, the edge pairs (A) (resp., (B)) determine 4-cycles (resp., 6-cycles). The subgraphs of $X_{r,t}^3$ induced by the $\binom{n}{r}$ cosets of $S_r \times S_t$ in S_n are the components of the subgraph $X_{r,t}^3 \setminus F_\epsilon$ of $X_{r,t}^3$, see Subsection 1.1. These components are copies of a cartesian product $\Pi_r^t = X_r^{d_r} \square X_t^{d_t}$ with: **(a)** $d_r = d_t = 2$, if $\min(r, t) > 2$; **(b)** $d_r = 2 = d_t + 1$, if $r > t = 2$; **(c)** $d_r = d_t = 1$, if $r = t = 2$.

If an α -E-set J of $X_{r,t}^3$ is equivalent in all copies of Π_r^t of $X_{r,t}^3$, than both J and its associated 1-sphere packing are said to be *uniform*. There is no uniform α -E-set in $X_{2,2}^3$, see Figure 1 below. Theorem 5.1 will show that if $4 < n = r + t$, then uniform α -E-sets of $X_{r,t}^3$ have $\alpha \leq \frac{n}{rt} < 1$. Theorem 8.1 and Corollary 8.2 will certify that such an upper bound $\frac{n}{rt}$ can only be attained by uniform α -E-sets that intersect each copy of Π_r^t in a product $J' \times J''$ of E-sets $J' \subset X_r^{d_r}$ and $J'' \subset X_t^{d_t}$. Then, all α -E-sets in the graphs $X_{r,t}^3$ happen with $\alpha < 1$ and Theorem 1.1 follows. Our plan of proof is complemented in Subsection 1.4.

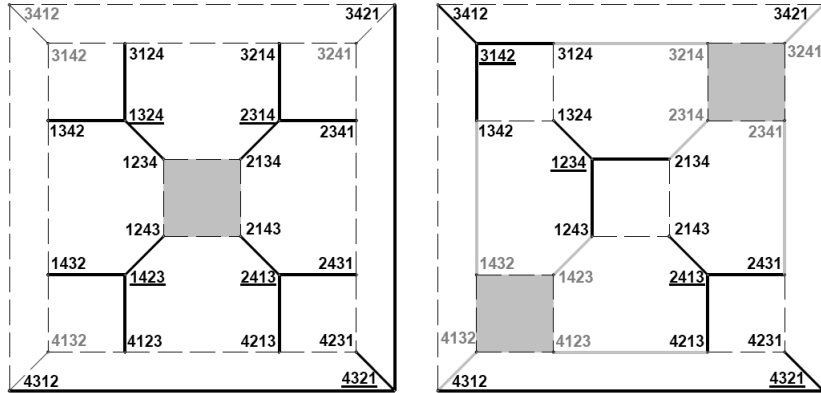


Figure 1. Representations of a $(5/6)$ - and a $(2/3)$ -E-set of $X_{2,2}^3$

Every α -E-set in $X_{2,2}^3$ avoids at least one of the six copies of Π_2^2 in $X_{2,2}^3$. See the two instances of α -E-sets in $X_{2,2}^3$ in Figure 1, with each avoided copy of Π_2^2 bounding a solid-gray square. On the left, the edges incident to a $(5/6)$ -E-set are in thick trace. (In expressing n -tuples in S_n , commas and parentheses are ignored). On the right, (to be compared with the construction in Section 6 and initiating the inductive construction of Section 7), a 1-sphere packing \mathcal{S} of $X_{2,2}^3$ is shown that covers $16 = (2/3)4!$ vertices, with underlined black 1-sphere centers. The 1-spheres of \mathcal{S} , forming a $(2/3)$ -E-set, induce the edges in thick black trace. Of the other edges, those colored (23) = (ϵ) , induced by the \mathcal{S} -spheres,

forming a \mathcal{T} as in Subsection 1.1, are in thick light-gray. The eight vertices in the \mathcal{S} -spheres of \mathcal{T} not in the 1-spheres of \mathcal{S} are light-gray (in contrast with the remaining vertices, in black) and span two 4-cycles bounding solid gray squares as cited above.

1.4. Largest Cayley Subgraph with an E-set

To obtain Theorem 8.1, we follow the following development in Sections 6–8. Let $r = t > 2$. In each copy of Π_r^t (Subsection 1.3) a partition of $S_r = V(X_r^{d_r})$ into E-sets (Subsection 1.2) is combined by concatenation with a corresponding partition of the subgroup $A_t = V(X_t^{d_t}[A_t])$ of index 2 in S_t . Now, a connected subgraph $X' = X'_{r,t}$ induced by 2^r of the $\binom{n}{r}$ copies of Π_r^t in $X_{r,t}^3$ has an E-set J . Here, X' is the largest subgraph of $X_{r,t}^3$ with a perfect 1-sphere packing. Also, $V(X')$ is a subgroup of S_n containing J as a subgroup. Theorem 8.1 implies that J , whose associated 1-sphere packing has maximum *localized packing density* (Section 6 and following), cannot be extended to an E-set of $X_{r,t}^3$. Moreover, J extends to a maximum nonuniform α -E-set of $X_{r,t}^3$ with largest $\alpha > \frac{n}{r^2}$ such that $\alpha < 1$. Corollary 8.2 allows to extend this case of $X_{r,r}^3$ to the case of $X_{r,t}^3$ ($r > t > 2$), via puncturing restriction. This allows the completion of the proof of Theorem 5.1, and thus that of Theorem 1.1.

Remark 1.2. A conjecture in [4] says that no E-set of X_n^d exists if $d > 2$. Remark 1 [3] says that a proof of this conjecture as “Theorem 5” [4] fails. This can be corrected for $d > 2$ by restricting to either $n = 4$ or n a prime $n > 4$, proved in [3] for path graphs τ^d . It can be proved for any tree τ^d using [4] Lemma 6 that generalizes the decomposition of $X_{r,t}^3 \setminus F_\epsilon$ in Subsection 1.3.

2. JOHNSON GRAPHS

Let $2 < r < n - 1$ in \mathbb{Z} . Let $\Gamma_n^r = (V, E)$ be the edge-colored graph with $V = \{r\text{-subsets of } I_n\}$ and $tu \in E \Leftrightarrow t \cap u$ is an $(r - 1)$ -subset, said to be the *color* of tu . Note that Γ_n^r is the Johnson graph $J(n, r, r - 1)$ [7]. A subgraph Ψ of Γ_n^r is *exact* if: (a) each two of its edges incident to a common vertex have the $(r - 1)$ -subsets representing their colors sharing exactly $r - 2$ elements of I_n , and (b) the vertices u, v, w of each $P_3 = uvw$ in Ψ involve $r + 2$ elements of I_n , that is: $|u \cup v \cup w| = r + 2$. Exact spanning subgraphs Φ_n^r of Γ_n^r are applied in Sections 3–5 to packing 1-spheres into $X_{r,t}^3$.

An exact cycle in Γ_5^3 is $\psi_5 = (345, 234, 123, 512, 451)$ (or in reverse, $\psi_5^{-1} = (321, 432, 543, 154, 215)$), where each triple $a_0a_1a_2$ acquires the element a_0 among those absent in the preceding triple and loses the element a_2 among those present in the following triple, with 3-strings taken cyclically mod 5. This is also expressed as a *condensed cycle* (or *CC*) of triples $\psi_5 = (12345)$, (resp., $\psi_5^{-1} = (54321)$),

whose successive composing triples yield corresponding successive terms of the original form of ψ_5 , (resp., ψ_5^{-1}). We can take an exact $\Phi_5^3 \in \{\{\psi_5, \psi'_5\}, \{\psi_5^{-1}, \psi'^{-1}_5\}, \{\psi_5, \psi'^{-1}_5\}, \{\psi_5^{-1}, \psi'_5\}\}$, where

$$(1) \quad \begin{aligned} \psi_5 &= (345, 234, 123, 512, 451) = (12345), \psi'_5 = (135, 413, 241, 524, 352) = (13524), \\ \psi_5^{-1} &= (321, 432, 543, 154, 215) = (54321), \psi'^{-1}_5 = (142, 314, 531, 253, 425) = (53142), \end{aligned}$$

are expressed as cycles of triples in Γ_5^3 and as their respective CCs.

3. APPLICATION TO SPHERE PACKING

The exact 2-factor above combine with the decomposition of $X_{r,t}^3 \setminus F_\epsilon$ into copies of Π_r^t in Subsection 1.3. In preparation for Theorem 5.1, we provide an example.

31245 32145 12345 13245 23145 21345	15342 13542 53142 51342 31542 35142
31254 32154 12354 13254 23154 21354	15324 13524 53124 51324 31524 35124
34251 32451 42351 43251 23451 24351	14325 13425 43125 41325 31425 34125
34215 32415 42315 43215 23415 24315	14352 13452 43152 41352 31452 34152
34512 35412 45312 43512 53412 54312	14253 12453 42153 41253 21453 24153
34521 35421 45321 43521 53421 54321	14235 12435 42135 41235 21435 24135
14523 15423 45123 41523 51423 54123	54231 52431 42531 45231 25431 24531
14532 15432 45132 41532 51432 54132	54213 52413 42513 45213 25413 24513
12534 15234 25134 21534 51234 52134	53214 52314 32514 35214 25314 23514
12543 15243 25143 21543 51243 52143	53241 52341 32541 35241 25341 23541

Figure 2. A uniform (5/6)-E-set in $X_{3,2}^3$ via an exact Φ_5^3

Note that $X_{3,2}^3 \setminus F_\epsilon$, (where $(34) = (\epsilon)$), splits into ten copies of $\Pi_3^2 = X_3^2 \square X_2^1$. Each 2×6 array in Figure 2 shows one such copy, composed by: (i) two copies of X_3^2 (shown as contiguous rows), i.e. two 6-cycles (obtained in the upper-left corner, by concatenating 45 or 54 to each entry of $(312, \xi_3^1, 321, \xi_2^2, 123, \xi_1^1, 132, \xi_3^2, 231, \xi_2^1, 213, \xi_1^2)$, with edges represented by the copies ξ_j^i of X_2^1 , using Subsection 1.2); (ii) six column-wise copies of X_2^1 ; (iii) six 4-cycles given by contiguous columns. The five copies of Π_3^2 on the left of the figure are in ordered correspondence with the terms of the 5-cycle $\psi_5^{-1} = (321, 432, 543, 154, 215)$ in display (1): the black vertices in each of the five copies of Π_3^2 determine two 1-spheres with the two dark-gray vertices in the subsequent copy of Π_3^2 , where: (a) the top copy of Π_3^2 is taken to be subsequent to the bottom copy; (b) the center of each such 1-sphere is underlined; (c) one of the two underlined vertices in each copy of Π_3^2 starts with the triple given by a corresponding term in ψ_5^{-1} ; and (d) the remaining vertices are light-gray. For example, a 1-sphere here is given by the underlined-black vertex 32145 (forming part of the product $J = \xi_1^3 \times \xi_4^4 = (12)3 \times 4(5)$

of E-sets in $\Pi_3^2 = X_3^2 \square X_2^1$) in the top copy of Π_3^2 , its black neighbors 12345, 31245 and 32154 and the dark-gray vertex 32415 in the subsequent copy of Π_3^2 . Similarly, the five copies of Π_3^2 on the right of Figure 2 are linked to the 5-cycle $\psi'_5 = (135, 413, 241, 524, 352)$. Now, the underlined vertices yield a (5/6)-E-set.

4. CYCLIC ORDERED PARTITIONS

No exact 2-factor Φ_6^4 exists. This is remedied in (B) below. On the other hand, an exact 2-factor Φ_7^4 is given by the CCs $\phi_1 = (1234567)$, $\phi_2 = (1357246)$, $\phi_3 = (1473625)$, that we equalize to the respective *cyclic ordered partitions* (or COPs) $1114 = \phi_1$, $2221 = \phi_2$, $1213 = \phi_3 = \{1245 = 2514, 2356 = 3627, \dots, 7134 = 1473\}$ of the integer 7 (associated with the successive difference triples 111, 222, 333 of quadruples) and by alternating the quadruples in the COPs

$$\begin{aligned} 1123 &= \{1235, 2346, 3457, 4561, 5672, 6713, 7124\}, \\ 2113 &= \{1345, 2456, 3567, 4671, 5712, 6123, 7234\}, \end{aligned}$$

into the exact CC $(1235, 1345, 4561, 4671, 7124, 7234, 3457, 3567, 6713, 6123, 2346, 2456, 5672, 5712)$. Note that Γ_7^5 has COPs $11113 = \phi_1$, $11122 = \phi_2$ and $11212 = \phi_3$, yielding an exact Φ_7^5 .

Exact spanning subgraphs of largest degree 3 in Γ_n^r whose components are unicyclic caterpillars, (i.e. graphs for which the removal of its pendant vertices makes them cyclic) will be called *nests*. Then, a nest leads to a uniform α -E-set with $\alpha = \frac{n}{rt}$. For example: (A), the nest of Γ_5^3 formed by the CC (12345) plus the edges $(132, 135)$, $(423, 421)$, $(354, 352)$, $(415, 413)$ and $(251, 254)$ leads to a uniform $(5/6)$ -E-set; (B) In Γ_6^4 , the COPs 1113 and 1122 alternate into the exact 12-cycle

$$(1234, 1235, 2345, 2346, 3456, 3451, 4561, 4562, 5612, 5613, 6123, 6124).$$

A nest is obtained by attaching edges with pendant vertices in the COP $1212 = \{1245, 2356, 3461\}$, say edges $(1235, 1245)$, $(3451, 3461)$ and $(5613, 2356)$. This leads to a uniform $(1/4)$ -E-set in $X_{4,2}^3$; an alternate nest of Γ_6^4 is formed by the 5-cycles

$$\begin{aligned} (12345)|6 &= (1236, 2346, 3456, 4516, 5126) \\ (62413)|5 &= (6245, 2415, 4135, 1365, 3625) \end{aligned}$$

plus the edges $(6245, 1246)$, $(2415, 1234)$, $(4135, 5234)$, $(1365, 1346)$, $(3625, 5123)$.

For $n > 4$, exact non-spanning subgraphs of Γ_n^r yield $\alpha < \frac{n}{rt}$. To exemplify this, we reselect the centers of disjoint 1-spheres in Figure 2 by taking all vertices in a copy of Π_r^t as dark-gray and its neighbors via F_ϵ underlined-black, then setting as dark-gray enough vertices at distance 2 from underlined-black vertices, traversing F_ϵ to set underlined-black vertices in all copies of Π_r^t . One can select more than one copy of Π_r^t to be completely dark-gray, e.g. those copies containing

vertices 123456 and 654321 in $X_{3,3}^3$ and proceed as above until the twenty copies of Π_r^t have underlined-black vertices, but the value of α in such cases is still less than $\frac{n}{rt}$.

5. UNIFORM SPHERE PACKING

Assume $4 < n = r + t$, where $r, t \in \mathbb{Z}$. Then each copy Π' of $\Pi_r^t = X_r^{d_r} \square X_t^{d_t}$ in $X_{r,t}^3$, where $d_r, d_t \in \{1, 2\}$, has $r!t!$ vertices. We use now from Sections 6-8 below that covering a copy Π' with 1-spheres of a packing \mathcal{S} of $X_{r,t}^3$ prevents \mathcal{S} for being uniform. As a consequence, it arises from Sections 3-4 that uniform α -E-sets J in $X_{r,t}^3$ have $\alpha \leq \frac{n}{rt}$, as their intersection with each Π' is contained at most in a product of E-sets, guaranteeing $\alpha \leq \frac{n}{rt}$. Moreover, if $\alpha = \frac{n}{rt}$ then each $\Pi' \cap J$ equals $J' \times J''$. Here, J' and J'' are E-sets in $X_r^{d_r}$ and $X_t^{d_t}$ of the forms ξ_i^r ($1 \leq i < r$) and $\xi_j^{r^*}$ ($r^* < j \leq n$) respectively, (instead of $\xi_i^1 = i(I_n \setminus \{i\})$ with $1 < i \leq n$, as in Subsection 1.2). Let $N[J' \times J'']$ be the union of the 1-spheres centered at the vertices of $J' \times J''$. Then $\Pi' - N[J' \times J'']$ is the disjoint union of $(r-1)(t-1)$ copies of Π_{r-1}^{t-1} . Also, each Π' intersects J in $(r-1)!(t-1)!$ vertices. These are the centers of pairwise disjoint 1-spheres, yielding a total of $(r-1)!(t-1)!n$ vertices in all those spheres. This way, $\frac{n}{rt}n!$ vertices of $X_{r,t}^3$ become covered by pairwise disjoint 1-spheres in $X_{r,t}^3$. This together with the outcome of Subsection 1.4 yields a maximal imperfect uniform 1-sphere packing of $X_{r,t}^3$. Such a packing ensures the nonexistence of E-sets of $X_{r,t}^3$ via the arguments of Theorem 8.1 and Corollary 8.2 below.

Theorem 5.1. *Let $4 < n = r+t$, $(r, t \in \mathbb{Z})$. Then, there are at most $\frac{n}{rt}n!$ vertices in the union of 1-spheres of an imperfect uniform 1-sphere packing of $X_{r,t}^3$. This ensures the nonexistence of E-sets of $X_{r,t}^3$.*

6. LOCALIZED PACKING DENSITY

The techniques in this and following sections lead to maximum *localized packing density*, meaning the packing of as many 1-spheres as possible in a specific copy of Π_r^t according to the decomposition of $X_{r,t}^3 \setminus F_\epsilon$ in Subsection 1.3.

To start with, a 1-sphere packing \mathcal{S} of $X_{3,3}^3$ is indicated in Figure 3 that contains in the fashion of Figure 2 eight 6×6 arrays each standing for the disposition of vertices in an embedding of a copy of Π_3^3 in a torus. In each such array, the black 6-tuples represent centers of 1-spheres in \mathcal{S} . There are two such centers in the first, (resp., third), [resp., fifth] row, namely in columns 1 and 4, (resp. 3 and 6), [resp., 5 and 2]. Each dark-gray 6-tuple stands for a vertex adjacent to one of the said 1-sphere centers located in a different copy of Π_3^3 via transposition $(\epsilon) = (34)$. There are two of these dark-gray 6-tuples: in the second, (resp., fourth), [resp., sixth] row of each 6×6 array, namely in columns 2 and 5, (resp.,

123456 132456 231456 213456 312456 321456	246135 264135 462135 426135 624135 642135
123546 132546 231546 213546 312546 321546	246315 264315 462315 426315 624315 642315
123645 132645 231645 213645 312645 321645	246513 264513 462513 426513 624513 642513
123465 132465 231465 213465 312465 321465	246153 264153 462153 426153 624153 642153
123564 132564 231564 213564 312564 321564	246351 264351 462351 426351 624351 642351
123654 132654 231654 213654 312654 321654	246531 264531 462531 426531 624531 642531
214365 241365 142365 124365 421365 412365	154326 145326 541326 514326 415326 451326
214635 241635 142635 124635 421635 412635	154236 145236 541236 514236 415236 451236
214536 241536 142536 124536 421536 412536	154632 145632 541632 514632 415632 451632
214356 241356 142356 124356 421356 412356	154362 145362 541362 514362 415362 451362
214653 241653 142653 124653 421653 412653	154263 145263 541263 514263 415263 451263
214563 241563 142563 124563 421563 412563	154623 145623 541623 514623 415623 451623
326154 362154 263154 236154 632154 623154	365214 356214 653214 635214 536214 563214
326514 362514 263514 236514 632514 623514	365124 356124 653124 635124 536124 563124
326415 362415 263415 236415 632415 623415	365421 356421 653421 635421 536421 563421
326145 362145 263145 236145 632145 623145	365241 356241 653241 635241 536241 563241
326541 362541 263541 236541 632541 623541	365142 356142 653142 635142 536142 563142
326451 362451 263451 236451 632451 623451	365412 356412 653412 635412 536412 563412
135246 153246 351246 315246 513246 531246	456123 465123 564123 546123 645123 654123
135426 153426 351426 315426 513426 531426	456213 465213 564213 546213 645213 654213
135624 153624 351624 315624 513624 531624	456312 465312 564312 546312 645312 654312
135264 153264 351264 315264 513264 531264	456132 465132 564132 546132 645132 654132
135462 153462 351462 315462 513462 531462	456231 465231 564231 546231 645231 654231
135642 153642 351642 315642 513642 531642	456321 465321 564321 546321 645321 654321

Figure 3. Local maximum packing density in $X_{3,3}^3$

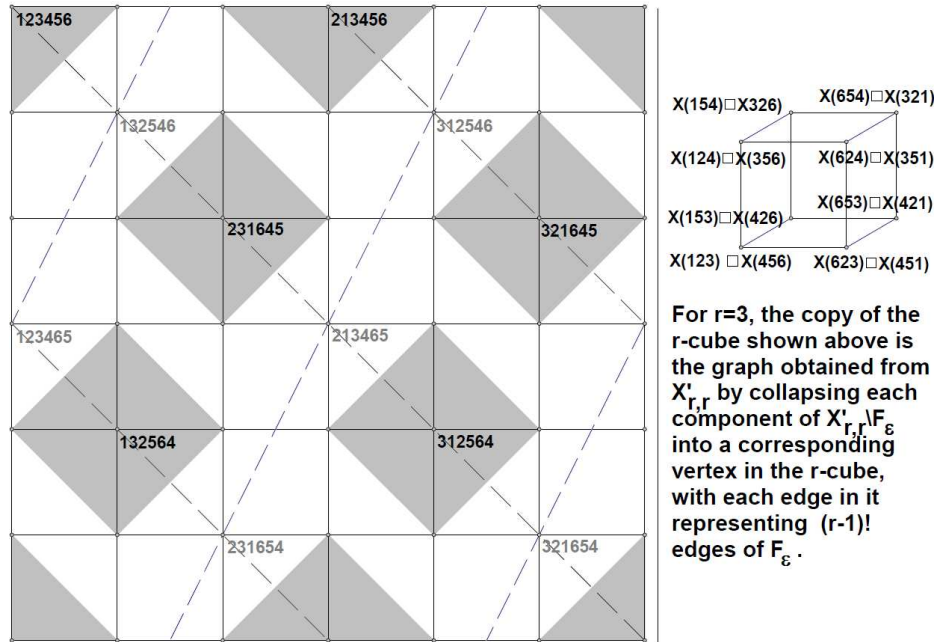


Figure 4. Embedding of $X(123) \square X(456)$ in a torus and a representation of $X'_{3,3}$

4 and 1), [resp., 6 and 3]. This divides the black and dark-gray 6-tuples in each 6×6 array into three 2×2 sub-arrays obtained from the diagonal black 6-tuples by transpositions (12) and (56) and their composition. The left and center of Figure 4 represents, with the same 6-tuple shades of Figure 3, its upper-left copy of Π_3^3 , namely $X(123)\square X(456)$.

TABLE I

$X(123)\square X(456)$	123456	213456	312564	132564	231645	321645
$X(214)\square X(365)$	214365	124365	421653	241653	142536	412536
$X(326)\square X(154)$	326154	236154	632541	362541	263415	623415
$X(135)\square X(246)$	135246	315246	513462	153462	351624	531624
$X(246)\square X(135)$	246135	426135	624351	264351	462513	642513
$X(154)\square X(326)$	154326	514326	415263	145263	541632	451632
$X(365)\square X(214)$	365214	635214	536142	356142	653421	563142
$X(456)\square X(123)$	456123	546123	645231	465231	564312	645312

TABLE II

$X(162)\square X(534)$	162534	612534	162543	612543
$X(165)\square X(234)$	165234	615234	165243	615243
$X(163)\square X(425)$	163425	613425	163452	613452
$X(164)\square X(325)$	164325	614325	164352	614352
$X(256)\square X(134)$	256134	526134	256143	526143
$X(251)\square X(634)$	251634	521634	523416	521643
$X(254)\square X(316)$	524361	254361	524316	254316
$X(253)\square X(416)$	523461	523461	523416	523416
$X(431)\square X(652)$	431652	341652	431625	341652
$X(436)\square X(152)$	436152	346152	436125	346152
$X(432)\square X(516)$	432516	342516	432561	342561
$X(435)\square X(216)$	435216	345216	435261	345261

Table I lists on its leftmost column the copies of Π_3^3 of Figure 3, followed to their right by three pertaining pairs of 6-tuples encodable as $(a_{i,1}, a_{i,2}, a_{i,3})$, where $i \in I_8$. For instance, $a_{1,1} = \{123456, 213456\}$, $a_{1,2} = \{312564, 132564\}$, etc. Consider the following pairs of pairs of black 6-tuples in the main diagonals of the eight 6×6 arrays in Figure 3 related by the permutation (12)(34)(56):

$$(2) \quad \begin{aligned} & \{a_{1,1}, a_{2,1}\}, \{a_{1,2}, a_{4,1}\}, \{a_{1,3}, a_{3,1}\}, \{a_{2,2}, a_{5,1}\}, \{a_{2,3}, a_{6,2}\}, \{a_{3,2}, a_{7,1}\}, \\ & \{a_{3,3}, a_{5,2}\}, \{a_{4,2}, a_{6,1}\}, \{a_{4,3}, a_{7,2}\}, \{a_{5,3}, a_{8,2}\}, \{a_{6,3}, a_{8,1}\}, \{a_{7,3}, a_{8,3}\}. \end{aligned}$$

The eight copies of Π_3^3 in Figure 3 induce a subgraph $X'_{3,3}$ of $X_{3,3}^3$ (right of Figure 4) whose vertex set admits a partition into 48 1-spheres around the black 6-tuples, with a partial total of 288 vertices. Moreover, $X'_{3,3}$ has an E-set J formed by the black 6-tuples, encoded in the pairs of display (2). Consider the vertices of the remaining 12 copies of Π_3^3 in $X_{3,3}^3$ at distance 2 from a center of a 1-sphere among the cited 48. There are 192 such vertices, 16 in each of the 12

copies as the union of four copies of a product $J' \times J''$ of E-sets as in Section 5 and inducing four 4-cycles in the copy. The graph induced by the remaining 20 vertices in the copy contains four 1-spheres whose vertices via F_ϵ are centers of similar 1-spheres. As a result we have the formation of double spheres, see below. Table II allows to select 24 centers of pairwise disjoint 1-spheres to cover half of the resulting $240 = 12 \times 20$ vertices: choose one 1-sphere center per pair of two 6-tuples in each box in the table. There are 144 vertices in the 24 1-spheres. In sum, we obtain $\frac{3}{5}6!$ vertices of $X_{3,3}^3$ packed into $72 = 48 + 24$ 1-spheres.

Let us apply the definitions of double-sphere and \mathcal{S} -sphere in Subsection 1.1 with $X = X_{3,3}^3$ and $X' = X'_{3,3}$. By adding to each 1-sphere Σ in the above packing of X' the end-vertices of the (ϵ) -colored edges departing from Σ , where $(\epsilon) = (34)$, a corresponding \mathcal{S} -sphere Σ' is obtained enlarging Σ . On the other hand, the 24 1-spheres selected above can be extended into 24 double-spheres, which forms a double-sphere packing. A transformation of the 1-sphere packing \mathcal{S} in Figure 3 into a perfect special (Subsection 1.1) packing of $X_{r,t}^3$ is obtained by enlarging the 48 1-spheres that pack perfectly X' into corresponding \mathcal{S} -spheres by adding the 192 vertices not in X' and at distance 2 from the centers of the 48 1-spheres. The reader may compare this with the \mathcal{S} -sphere packing of $X_{2,2}^3$ suggested on the right of Figure 1.

Selecting instead 24 centers of 1-spheres to be the neighbors via the transposition (23) (or (13)) of the 24 centers allowed above by means of Table II leaves room to selecting additional 24 centers of 1-spheres in the six still untouched copies of Π_3^3 . The selection of the 24 new centers of 1-spheres in those six copies must be done via the transposition (45) (or (46)). This yields a packing of $X_{3,3}^3$ by 96 1-spheres comprising $576 = \frac{4}{5}|V(X_{3,3}^3)|$ vertices. Observe that the 96 corresponding centers are obtained by modifying the original 1-sphere centers both adjacently and alternatively, idea to be generalized in Theorems 8.1.

7. RENUMBERING TREE VERTICES

In generalizing the maximum localized packing density of Section 6, we found it convenient to modify the order of vertices of the tree $\tau_{r,t}^3$ in items (i)-(ii) of Subsection 1.3 by letting instead: (i') 1 and $r^* = r + 1$ denote the vertices of respective degrees r and t in $\tau_{r,t}^3$ so that $\epsilon = 1r^*$; (ii') 2, ..., r (resp., $r^* + 1, \dots, n$) denote the vertices adjacent to vertex 1 (resp., r^*) in $\tau_{r,t}^3$.

We exemplify this modification via Figure 5, on whose top a representation of the copy $X(12) \square X(34)$ of Π_2^2 is given that presents, before and after (symbol) \square , the copies of K_2 constituting $X(12)$ and $X(34)$, respectively. Similar representations can be given for $X(32) \square X(14)$, $X(14) \square X(32)$ and $X(34) \square X(12)$, forming with $X(12) \square X(34)$ a subgraph $X'_{2,2}$ of $X_{2,2}^3$ preceding the subgraph $X'_{3,3}$ of $X_{3,3}^3$ in Section 6. The two remaining squares $X(13) \square X(24)$ and $X(24) \square X(13)$ are

shaded in light-gray color in Figure 1 (that used the original vertex numbering in items (i)-(ii), Subsection 1.3) and form a second subgraph $X''_{2,2}$ of $X^3_{2,2}$.

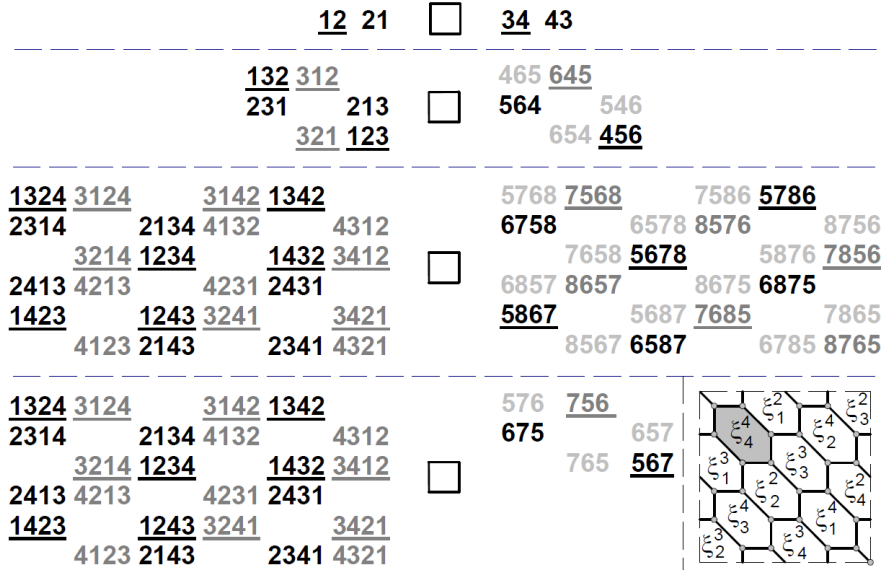


Figure 5. Interpretations of Π_2^2 , Π_3^3 , Π_4^4 and Π_4^3

Subsequently in Figure 5, a similar representation of the cartesian product $X(123)\square X(456)$ is given that shows, before and after \square , the 6-cycles $X(123)$ and $X(456)$, respectively, by presenting adjacent vertices contiguously: horizontally, vertically and diagonally between upper-left and lower-right. Here, the black centers of the three 1-spheres in the main diagonal of the 6×6 array representing $X(123)\square X(456)$ in Figure 3 (but with the vertex order assumed above in this section) are recovered by: **(A)** taking a partition of $V(X(123))$ into the E-sets $\xi_1^1 = 1(23)$, $\xi_2^1 = 2(13)$, $\xi_3^1 = 3(12)$ (Subsection 1.2) given by: **(i)** underlined-black color for $\xi_1^1 = \{123, 132\}$, **(ii)** (not underlined) black color for $\xi_2^1 = \{213, 231\}$ and **(iii)** underlined-dark-gray color for $\xi_3^1 = \{312, 321\}$; **(B)** assigning the three colors of (A) respectively to the even-parity vertices in $X(456)$ as follows: **(i)** $456 \in \xi_4^4$, **(ii)** $564 \in \xi_5^4$ and **(iii)** $645 \in \xi_6^4$, while the odd-parity vertices, namely 465 , 546 and 654 , shown in light-gray, do not intervene; **(C)** concatenating the vertices of $X(123)$ and $X(456)$ having a common color.

Now, we embed each copy of X_4^2 into a torus, as in the lower-right corner of Figure 5, with its copies ξ_i^j , $(j \in \{2, 3, 4\}; i \in I_4)$, of X_3^2 presented as above into their places. This way, the previous representation of $X(123)\square X(456)$ is extended to Π_4^4 as in the lower two instances of Figure 5, where the shown cartesian products can be denoted $X(1234)\square X(5678)$ and $X(1234)\square X(567)$, this one obtained by restricting, i.e. puncturing $X(1234)\square X(5678)$.

In the third case of Figure 5, the coloring used for $X(123)\square X(456)$ above is extended with a fourth color: (not underlined) dark-gray. On the left of \square , the colors correspond to the E-sets $\xi_i^1 = i(I_4 \setminus \{i\})$, where $i \in I_4$. On the right of \square , the even-parity 4-tuples are given the same color i when their intersection with an E-set of the partition $\{\xi_j^5; j = 5, 6, 7, 8\}$ starts with $j = i + 4$. As mentioned, the situation for $X(1234)\square X(567)$ can be considered a restriction of that of $(1234)\square X(5678)$. We may write $X(567) = (567, \xi_7^7, 657, \xi_5^6, 756, \xi_5^6, 6576, \xi_7^6, 675, \xi_5^7, 765, \xi_6^6)$.

In a typical cartesian product $\Pi_r^t = X_r^2 \square X_t^2$, where $2 < t \leq r$, we notice that: **(A)** the subset Q of vertices of the copy $X(r^* \cdots n)$ of X_t^2 , where $r^* = r + 1$, which as t -tuples have the same parity as the t -tuple $r^* \cdots n$ has a partition into t subsets Q_i with the t -tuples in Q_i starting at $(r + i)$, for every $i \in I_t$; **(B)** the vertex set of the copy $X(1 \cdots r)$ of X_r^2 has a partition into the r E-sets ξ_j^1 for every $j \in I_r$; **(C)** it eases treatment to consider the n -tuples obtained by concatenating every r -tuple in ξ_i^1 with every t -tuple in Q_i , for every $i \in I_t$.

The convenience of the new vertex numbering is that to obtain a maximal number of disjoint 1-sphere centers in the copies of Π_r^t , say $X(1 \cdots r)\square X(r^* \cdots n)$, we can order both factors of these products in the same direction, resulting in transpositions between the first entry of either an initial r - or a terminal t -tuple with any of the remaining entries of that tuple, plus the transposition of both first entries. We concatenate initial r -tuples and terminal t -tuples whenever they have the same color (as in the instances of Figure 5), where the color set of the second factor in the product must coincide with, or be contained in, the color set of the first factor, considering that the second coloring here is given on the elements of the alternate subgroup $A_t \subset S_t$ while the first coloring is taken from a partition of S_r into E-sets.

8. NONUNIFORM SPHERE PACKING

TABLE III

$r; k$	0	1	2	3	...	Σ_r	$r; k$	0	1	2	3	...	Σ'_r
2	4	2	—	—	...	6	2	4	0	—	—	...	4
3	8	12	—	—	...	20	3	8	8	—	—	...	16
4	16	48	6	—	...	70	4	16	24	0	—	...	40
5	32	160	60	—	...	252	5	32	64	24	—	...	120
6	64	480	360	20	...	924	6	64	160	120	0	...	344
7	128	1344	1680	280	...	3432	7	128	384	480	80	...	1072
...

Let $r > 1$. If $z, z' \in I_n$ with $|z - z'| = r$, we denote $\mathbf{z} = \{z, z'\}$. There are 2^r copies of Π_r^r of the form $\Pi_r^r = X(a_1 a_2 \cdots a_r) \square X(a'_1 a'_2 \cdots a'_r)$ with $\mathbf{a}_i = \{a_i, a'_i\} = \{i, r + i\} = \mathbf{i}$, for $i \in I_r$. The subgraph $X'_{r,r}$ induced by these copies possesses an E-set J constructed as in Sections 6–7. Here, J also dominates a subset $\{y_1 b_2 \cdots b_r y_r d_2 \cdots d_r \mid \{b_2, \dots, b_r\} = \{y'_1, y_2, \dots, y_{r-1}\}; \{d_2, \dots, d_r\} =$

$\{y'_r, y'_2, \dots, y'_{r-1}\}\}$ in each copy of Π_r^r of the form $\Pi_r^r = X(y_1 y'_1 y_2 \cdots y_{r-1}) \square (y_r y'_r y'_2 \cdots y'_{r-1})$ in $X_{r,r}^3$ with $y_z \in \mathbf{y}_z$ for $z \in I_r$ and $\{\mathbf{y}_z \mid z \in I_r\} = \{\mathbf{z} \mid z \in I_r\}$. The $\binom{2r}{r}$ copies of Π_r^r in $X_{r,r}^3$ are of the following types:

$$(3) \quad \begin{array}{ll} X(a_1 a_2 \cdots a_r) & \square \quad X(a'_1 a'_2 \cdots a'_r); \\ X(a_1 a'_1 a_3 a_4 \cdots a_r) & \square \quad X(a_2 a'_2 a'_3 a'_4 \cdots a'_r); \\ X(a_1 a'_1 a_2 a'_2 a_5 a_6 \cdots a_r) & \square \quad X(a_3 a'_3 a_4 a'_4 a'_5 a'_6 \cdots a'_r); \\ \dots & \dots \\ X(a_1 a'_1 \cdots a_k a'_k a_{2k+1} a_{2k+2} \cdots a_r) & \square \quad X(a_{k+1} a'_{k+1} \cdots a_{2k} a'_{2k} a'_{2k+1} a'_{2k+2} \cdots a'_r); \\ \dots & \dots \end{array}$$

Let $X'_{r,r}, X''_{r,r}, X'''_{r,r}, \dots, X^{(k^*)}_{r,r}, \dots$ be the subgraphs induced respectively by the types in the first, second, third, \dots , k^* -th, \dots lines of display (3), where $k^* = k+1$. The number of times each $X^{(k^*)}_{r,r}$ occurs in $X_{r,r}^3$ is given by the sequence A051288 [13], presentable as a number triangle T each of whose terms $T(r, k)$, read by rows ($r \geq 0; k = 0, 1, \dots, \lfloor r/2 \rfloor$), $T(r, k)$, is the number of paths of r upsteps U and r downsteps D with exactly k subpaths UUD . In fact, $T(r, k) = \binom{r}{2k} 2^{r-2k} \binom{2k}{k}$. The left of Table III illustrates T , where each row of values $T(r, k)$ adds up to $\Sigma_r = \binom{2r}{r}$. Note F_ϵ has edges only between contiguous subgraphs $X^{(k)}_{r,r}$ and $x^{(k^*)}_{r,r}$, for $k = 0, 1, \dots, \lfloor r/2 \rfloor$.

In continuation to our approach in Sections 6–7. the right of Table III (the sum of which rows is indicated by Σ'_r) gives $(r!)^{-2}$ times the number of vertices covered by a maximum α -E-set K . The resulting quotient is denoted $S(r, k)$. Then, $S(r, k) \leq T(r, k)$. The intersection of such K and each copy of Π_r^r in $X_{r,r}^3 - X'_{r,r}$ is a product of two E-sets of X_r^2 by an argument extending that of the last three paragraphs of Section 6 that departs from the vertices in X'' at distance 2 from the E-set J constructed in X' . In fact, a copy Π' of P_r^r in $X''_{r,r}$ and an α -E-set extending J intersect at most in a product $J' \times J''$ of E-sets. We take the vertices of such $J' \times J''$ as centers of 1-spheres in Π' . These centers may appear in pairs of adjacent vertices in $X_{r,r}^3$ yielding a packing \mathcal{S}'' by double-spheres whose centers form a subset J^* . By displacing the vertices of J^* via alternate adjacency in the two components X_r^2 of each copy of Π_r^r in $X''_{r,r}$, we replace \mathcal{S}'' by a 1-sphere packing \mathcal{S}' containing $(2r) \times ((r-1)!)^2$ vertices of the $(r!)^2$ vertices of each copy of Π_r^r in $X''_{r,r}$, a proportion of $2/r$ of the vertices of $X''_{r,r}$. The same proportion is kept in the remaining $X''', \dots, X^{(k^*)}, \dots$, starting by choosing 1-spheres in the copies of Π_r^r in $X'''_{r,r}$ avoiding the neighbors (via F_ϵ) of the 1-spheres in \mathcal{S}' and then using “exact” paths in Johnson graphs as in Section 2.

Theorem 8.1. *If $n = 2r > 4$, where $r \in \mathbb{Z}$, then: (a) a connected subgraph $X'_{r,r}$ induced in $X_{r,r}^3$ by the disjoint union of 2^r copies of Π_r^r has a perfect 1-sphere packing \mathcal{S} ; (b) \mathcal{S} cannot be extended to a perfect 1-sphere packing of $X_{r,r}^3$; (c) a maximum nonuniform 1-sphere packing \mathcal{S}' of $X_{r,r}^3$ is obtained as an extension*

of \mathcal{S} that yields an α -E-set of $X_{r,r}^3$ with $\alpha = \Sigma'_r/\Sigma_r = (2^r + \frac{2}{r}P_r)/\binom{2r}{r}$, where $P_r = \binom{2r}{r} - 2^r$ if r is odd and $P_r = \binom{2r}{r} - 2^r - \binom{r}{r/2}$ if r is even; (d) $\frac{n}{r^2} < \alpha < 1$.

Proof. Apart from the 2^r copies of Π_r^r in $X_{r,r}'$ there are in $X_{r,r}^3$: $\binom{2r}{r} - 2^r$ copies of Π_r^r if r is odd and $\binom{2r}{r} - 2^r - \binom{r}{r/2}$ copies of Π_r^r if r is even. In these copies we could select products $\Upsilon = a(b_2 \cdots b_r).a'(c_2 \cdots c_r)$ formed by E-sets $a(b_2 \cdots b_r)$ and $a'(c_2 \cdots c_r)$. The cardinality of each such Υ is $((r-1)!)^2$, its vertices as centers of 1-spheres pairwise disjoint in their copies of Π_r^r but for F_ϵ possibly allowing the formation of pairwise disjoint double-spheres instead. As in the final discussion in Section 6 (presented with our initial notation, as in Table III), we could displace adjacently and alternatively the 1-sphere centers in the first and second components X_r^2 of Π_r^r . This can modify those double 1-spheres into pairwise disjoint 1-spheres which cover at best $2r((r-1)!)^2$ vertices of $X_{r,r}^3$. The number of times that $(r!)^2$ appears at most in the vertex counting of the resulting nonuniform packing of $X_{r,r}^3$ is $2^r + 2rP_r((r-1)!)^2/(r!)^2 = 2^r + 2rP_r/r^2 = 2^r + \frac{2}{r}P_r$. Thus, an α -E-set of $X_{r,r}^3$ has $\frac{n}{r^2} < \alpha \leq (2^r + \frac{2}{r}P_r)/\binom{2r}{r}$. This value of α is an $\alpha < 1$. \blacksquare

As in the bottom example of Figure 5, the general case of $X_{r,t}^3$ with $r \geq t$ can be considered a restriction, if necessary, of the one of $X_{r,r}^3$ by means of the puncturing technique mentioned in Section 7. This way, we get the following.

Corollary 8.2. *Let $r > t > 1$. A maximum nonuniform 1-sphere packing of $X_{r,t}^3$ exists that yields an α -E-set of $X_{r,t}^3$ with $\frac{n}{rt} < \alpha \leq \frac{\Sigma'_t}{\Sigma_r} < 1$, where $\Sigma'_t = (2^t + \frac{2}{t}P_t)$ and $\Sigma_r = \binom{2r}{r}$ with $P_t = \binom{2t}{t} - 2^t$ if t is odd and $P_t = \binom{2t}{t} - 2^t - \binom{t}{t/2}$ if t is even.*

REFERENCES

- [1] S. B. Akers and B. Krishnamurthy, *A group theoretic model for symmetric interconnection networks*, IEEE Trans. Comput., **38** (1989), 555–565.
- [2] S. Arumugam and R. Kala, *Domination Parameters of Star Graphs*, Ars Combinatoria, **44** (1996) 93–96.
- [3] S. Buzaglo and T. Etzion, *Bounds on the size of permutation codes with the Kendall τ -metric*, IEEE Trans. on Info. Theory, **61** (2015) 3241–3250.
- [4] I. J. Dejter, O. Serra, *Efficient dominating sets in Cayley graphs*, Discrete Appl. Math., **129** (2003), 319–328.
- [5] A. Ganesan, *An efficient algorithm for the diameter of Cayley graphs generated by transposition trees*, IJAM, **42** (2012), 214–233.

- [6] A. Ganesan, *Diameter of Cayley graphs of permutation groups generated by transposition trees*, JCMCC, **84** (2013), 29–40.
- [7] C. Godsil and G. Royle, Algebraic graph theory, Springer-Verlag, 2001.
- [8] T. W. Haynes, S. T. Hedetniemi, P. J. Slater, Fundamentals of Domination in Graphs, M. Dekker Inc., 1998.
- [9] G. A. Jones and J. M. Jones, Information and Coding Theory, Springer-Verlag, 2000.
- [10] A. V. Kelarev, J. Ryan, J. Yearwood, *Cayley graphs as classifiers for data mining: The influence of asymmetries*, Discrete Math., **309** (2009), 5360–5369.
- [11] A. V. Kelarev, *Labelled Cayley graphs and minimal automata*, Australasian J. Combinatorics, **30** (2004), 95–101.
- [12] A. V. Kelarev, Graph Algebras and Automata, M. Dekker, New York, 2003.
- [13] N. J. A. Sloane, The On-Line Encyclopedia of Integer Sequences, oeis.org.